Mesopore-Modified Zeolites: Preparation, Characterization, and Applications

Yousheng Tao,*,† Hirofumi Kanoh,† Lloyd Abrams,‡ and Katsumi Kaneko*,†

Department of Chemistry, Faculty of Science, Chiba University, Chiba 263, Japan, and DuPont Company, CR&D/CCAS, Experimental Station, Wilmington, Delaware 19880-0228

Received December 10, 2004

Contents

1. Introduction

The demand for environmentally friendly and more efficient technology has enhanced interest in the use and development of porous solids. These materials typically have high surface areas, which, coupled with their unique surface chemistries, offer unique reaction and adsorption selectivities. Zeolites are porous crystalline solids whose pores are of molecular dimensions thereby providing size and shape selectivity for guest molecules. Zeolites are widely used in catalysis as well as in the separation and purification fields due to their uniform, small pore size, high internal surface area, flexible frameworks, and controlled chemistry.[1−12] The major drawback of zeolites is that the small size of the channels (less than ∼0.8 nm) and cavities (typically <1.5 nm) imposes diffusional limitations on reactions that can cause high back pressure on flow systems.[12−16] It has been repeatedly demonstrated that mass transfer limitations play an important role in industrial applications using zeolites.[17−19] To circumvent the diffusional limitation imposed by zeolitic structures, several potential solutions have been explored:

- making zeolites with larger pores;
- making smaller zeolite particles;
- inserting larger pores into the zeolite particles.

Some effort was devoted to the development of zeolite materials with larger pores (>1.5 nm),[1,2] but the increases in pore size were modest. Further, these new materials are not very effective in reactions with large-sized molecules or for petroleum cracking reactions.[2]

The reduction of zeolite particle sizes has been employed as a means of reducing the intracrystalline diffusion path length.[20−33] However, as Camblor et al. reported, synthesizing zeolites with particle sizes below 100 nm caused a decrease in the micropore volume due to less perfect crystallization.[34,35] Other desirable properties are also affected; for example, filtration of the smaller zeolite particles is difficult due to their colloidal properties. For small particle zeolites, hydrothermal stability is reduced and considerable loss of crystallinity occurs during the activation dealumination process. The reduction in stabilty can be countered by synthesizing zeolite Y with a higher Si/Al ratio, but the activity decreases.[36,37]

Compared to the dimensions of the zeolite micropores (<2 nm), mesopores (2−50 nm) permit faster migration of guest molecules in the host frameworks. Since fast mass transfer of the reactants and products to and from the active sites is required for catalysts, the concept of infusing mesopores into zeolite particles has attracted much attention. This review covers articles published within the past five years describing different methods of creating and characterizing mesopores in zeolitic particles. The experimental conditions and pore structural parameters of mesoporous zeolites discussed in this review are included in the Summary as Table 1. The main approaches toward making mesopore-containing regular structures are as follows:

- direct synthesis;
- different postsynthesis treatments of zeolites using alkaline leaching, hydrothermal modification, and other chemical treatment;
- novel dual templating methods using carbon materials that are removed by oxidation.

2. Regular Mesoporous Silicates

New mesoporous organized silicates have been synthesized using a templating technique of which the Mobil MCM-41 is typical. MCM-41 exhibits a hexagonal arrangement of uniform mesopores whose dimensions can be engineered in the range of ∼1.5 nm to greater than 10 nm. Surfactant liquid crystals serve as organic templates linking the structure and pore dimensions of the MCM-41 materials to the structure of the surfactant, that is, chain length and solution chemis-

* To whom correspondence should be addressed. E-mail addresses: tao@pchem2.s.chiba-u.ac.jp (Y. Tao); kaneko@pchem2.s.chiba-u.ac.jp (K. Kaneko).
† Chiba University.
‡ DuPont Company, Publication No. 8685.

10.1021/cr040204o CCC: $59.00
Published on Web 01/31/2006

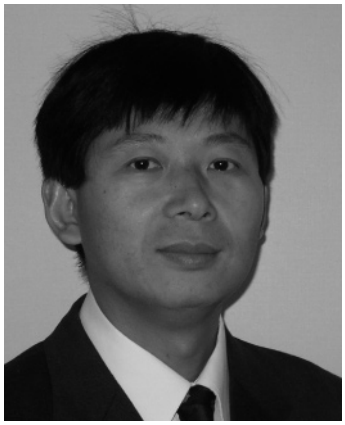

Yousheng Tao is originally from Hubei Province, China. He received his B.S. degree in Mineral Processing in 1987 from Wuhan Institute of Chemical Technology. He went to work for the Institute of Multipurpose Utilization of Mineral Resources, Chinese Academy of Geological Sciences, until 1991. He then went to Sichuan University, where he obtained his M.S. degree in Environmental Science and Engineering in 1993. After that, he worked in the Environmental Science Research Center, Xiamen University. Here he was promoted to senior engineer, was in charge of environmental engineering projects, and received several awards from Fujan provincial and Xiamen municipal governments for engineering achievements. He received a scholarship from the Japanese government and went to Japan in October, 2000. He earned his Ph.D, degree in Advanced Physical Chemistry in 2004 at Chiba University, Japan, under the supervision of Professor Katsumi Kaneko with a thesis on Mesoporosity-Donated Zeolites with Template Synthesis. He is currently working as a postdoctoral research fellow with Professor Katsumi Kaneko in the Department of Chemistry, Chiba University. His current research interests include the synthesis and characterization of nanoporous materials, study of nanosolutions with X-ray absorption fine structure (XAFS), and development of environmental protection techniques.

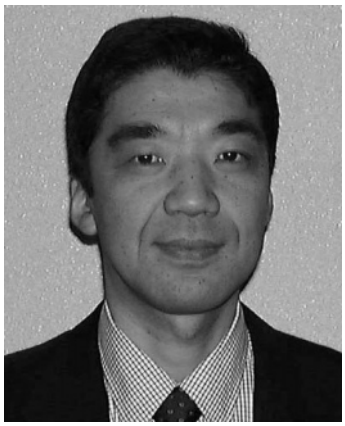

Hirofumi Kanoh was born in Gifu Prefecture of Japan in 1960. He studied chemistry from 1979 to 1986 at Nagoya University in Japan and obtained his M.Sc. in 1986 at the same university. Between 1986 and 2001, he worked as a researcher and a senior researcher at the Shikoku National Industrial Institute of AIST in Japan. Since 2001, he has been an associate professor of the Faculty of Science at Chiba University. His field of work concerns colloid and interface science, especially for nanoporous materials.

try.[38,39] The synthesis of these silica-based materials has promoted considerable interest, and since the original disclosure, there has been impressive progress in the development of many new mesoporous solids based on a similar mechanism of templating. For example, clay-based mesoporous solids designated as PCHs (porous clay heterostructures) were synthesized by the formation of MCM-like porous silica structures between clay layers.[40] A similar mesoporous silica was produced by folding the single layered polysilicate kanemite ($NaHSi_2O_5 \cdot 3H_2O$) sheet structures,

Lloyd Abrams has 37 years experience working in DuPont's Central Research and Development in the areas of adsorption phenomena, zeolites, microporous materials, catalysis, nanomaterials, and surface chemistry. He has worked with all DuPont business units and maintains research contacts with universities in Europe and Asia, as well as in the United States. Before joining DuPont, Lloyd's experience included the Apollo fuel cell project at Pratt & Whitney Aircraft, research and teaching assignments with Rutgers University, and a Postdoctoral Appointment at the Brookhaven National Laboratory. Lloyd graduated from the City College of New York in 1961 with a B.Ch.E. degree and then went to work for Pratt & Whitney Aircraft. In 1963, he began his Ph.D. studies at Rutgers University and, under the advisorship of Prof. Manfred J. D. Low, graduated in 1966 and then did a postdoctoral fellowship at Brookhaven under Dr. Augustine O. Allen. He began his career at DuPont in December, 1968. Among Lloyd's accomplishments are co-invention of five patents, publishing over 80 scientific papers, and serving as a frequent reviewer for professional journals. Within DuPont, he has received several Corporate awards for Engineering Excellence; external to DuPont, he has served on several Ph.D. thesis committees for Columbia University and the University of Delaware for Chemistry. In 1987, he was the Chairman of the Gordon Research Conference, *Chemistry at Interfaces.* He was a Special Peer Reviewer of the Shikoku National Industrial Research Institute, Shikoku, Japan, in 1999. He is a member of the American Chemical Society, the American Association for the Advancement of Science, and Sigma Xi.

Katsumi Kaneko is a professor of chemistry (physical chemistry), Faculty of Science, Chiba University. He has led a group of molecular chemistry since 1986 and continued to study gas adsorption on nanoporous materials with a variety of techniques. He published more than 290 papers. His study "Structures and reactivity of molecular assemblies in solid nanospaces" was awarded by the Chemical Society of Japan in 1999. He has been president of the International Adsorption Society and editor of *Adsorption Science and Technology* since 2004.

which is named FSM (folded sheets mesoporous materials) by Yanagisawa et al.[41,42]

Depending on the synthesis conditions, the silica source, and the type of surfactant used, other mesoporous materials were synthesized with thermal, hydrothermal, and mechanical

stability and mesostructures different from those of MCM, as recently reviewed by Linssen et al.[43] Briefly, HMS (hexagonal mesoporous silica) was prepared using hydrogen-bonding interactions and self-assembly between neutral primary amine micelles and neutral inorganic precursors. The ordered mesostructures have thicker framework walls, smaller crystallite domain size, and complementary textural mesoporosities in comparison with M41S materials templated by quaternary ammonium cations of equivalent chain length.[44−46] Mesoporous silica molecular sieve MSU (Michigan State University) was synthesized by the hydrolysis of tetraethyl orthosilicate in the presence of poly(ethylene oxide) (PEO) surfactants, the templating agents. By variation of the size and the structure of the surfactant molecules, disordered channel structures with uniform diameters ranging from 2.0 to 5.8 nm were obtained.[47−50] KIT (Korea Advanced Institute of Science and Technology) was synthesized using polymerization of silicate anions surrounding surfactant micelles in the presence of organic salts. The resulting pore structure was a three-dimensional, disordered network of short worm-like channels with uniform channel widths.[51] Well-ordered hexagonal mesoporous silica structures, SBA (Santa Barbara), with tunable large uniform pore sizes (up to ∼30 nm) were obtained by use of amphiphilic block copolymers as templating agents.[52−54] The thermal stability of these mesoporous materials was strongly related to their wall thickness and the silica precursor used during synthesis.[55]

Mesoporous silica materials with isomorphously substituted heteroatoms have been shown to exhibit considerable reactivity due to easily accessible active sites within their frameworks (heteroatoms inside the walls are not accessible).[1] Unfortunately, due to the amorphous nature of their frameworks and thin walls,[56,57] M41S-type mesoporous aluminosilicates collapse when they are mechanically compressed and have poor hydrothermal stability in boiling water and steam.[55,58−61] Gusev et al. showed that the ordered mesoporous structure of MCM-41 could be affected considerably by mechanical compression at pressures as low as 86 MPa and essentially destroyed at 224 MPa.[58] Cassiers et al. studied the thermal, hydrothermal, and mechanical stabilities of several mesoporous molecular sieves by means of X-ray diffraction and nitrogen adsorption and showed that none of the materials were especially stable and all materials collapsed at a pelletizing pressure of 450 MPa.[55] For reactions at lower temperatures than fluid cracking such as hydrocracking, hydrodesulfurization, and hydrodenitrogenation metal-supported MCM-41 catalysts have yielded good results owing to their high surface areas and regular pore dimensions.[62−65] Obviously, the lower stability (hydrothermal and mechanical) and reduced acidity of M41S materials compared to zeolites limit their practical applications. Since thermal, hydrothermal, and mechanical stabilities are critical parameters for potential applications, efforts have been made to improve the stability of M41S materials. Attempts have been made, unsuccessfully, to crystallize the pore walls of mesoporous materials.[9−11] Therefore, instead of upgrading the performance of individual mesoporous molecular sieves or zeolites, investigations have been undertaken to synthesize a new type of material that combines the advantages of each, namely, mesopore-modified zeolites. Some strategies have been developed to synthesize new materials that combine the advantages of mesoporous materials with those of zeolites, such as zeolite faujasite coated with a thin layer of mesoporous MCM-41,[66] incorporation of ZSM-5 within the framework walls of MCM-41, as well as ZSM-5/MCM-41 composites,[67−74] and MCM-41/β[75,76] and ZSM-5/MCM-48[77] composite materials, in which MCM-41, MCM-48, or SBA-15 is used as the mesostructural component.

Chen and Kawi tried to prepare a larger pore MFI-type zeolite by structural transformation of CTA^+−MCM-41 using CTA^+ (cetyltrimethylammonium) as the template.[78] Similarly, Hidrobo et al. reported stable zeolite-containing mesoporous aluminosilicates by incorporation of zeolite ZSM-5 generated within a mesoporous aluminosilicate.[79] The mesoporous aluminosilicates were hydrothermally synthesized from a hybrid organic−inorganic xerogel using a chitosan biopolymer as the template. In a subsequent step, zeolite ZSM-5 was produced in situ using tetrapropylammonium hydroxide as template and incorporated into the material. A general methodology was described by Trong On and Kaliaguine for the production of a new type of material with semicrystalline zeolitic mesopore walls.[80] This procedure involved a templated solid-state secondary crystallization of zeolites starting from amorphous SBA-15. The initially amorphous walls of the SBA-15 were progressively transformed into crystalline nanoparticles yielding improved hydrothermal stability. Nevertheless, these materials are still inferior to zeolites in terms of stability and acidity. These aluminosilicate mesostructures assembled from zeolite-type seeds such as zeolite Y, ZSM-5, and zeolite β did not show crystalline features by X-ray diffraction patterns. These materials are probably composed of an amorphous silica−alumina matrix with small zeolite particles either on its surface or within the pores.[68,69,79,81] Further discussion of such materials is beyond the scope of this review.

3. Mesopore-Modified Zeolites

Creation of mesopores in zeolite particles to increase accessibility to the internal surface has been the subject of many studies. It is known that postsynthesis hydrothermal dealumination and other chemical treatments form defect domains of 5−50 nm (which are attributed to mesopores) in faujasites, mainly zeolite Y.[82] Several dual templating methods for the preparation of mesoporous zeolite materials have been proposed:

- macrotemplating—using carbon black particles for preparing ZSM-5 of a wide pore size distribution (10−100 nm) or using monodispersed polystyrene spheres for preparing macroporous, ∼250 nm, silicates;[83−85]
- nanocasting—using colloid-imprinted carbons as templates for preparing small ZSM-5 particles with some interparticle mesopores.[86]

Jacobsen et al. prepared 12−30 nm mesoporous ZSM-5 by impregnating the synthesis gel components with multiwall carbon nanotubes.[87,88] Using carbon aerogel templating, Tao et al. synthesized uniform mesopore-modified ZSM-5 and Y zeolites.[89,90] The exploitation of templates in making mesoporous zeolites has clearly been receiving a great deal of attention for those working in zeolite synthesis.[91−93] Since mesopore-modified zeolites have shown promising properties (activity and selectivity) in catalytic processes, the next portion of this contribution deals with the hottest current topics and important progress in this field.

3.1. Leaching with NaOH Solution

Leaching with NaOH solution was recently applied to create mesopores in MFI zeolite.[16,94−103] In contrast to acid

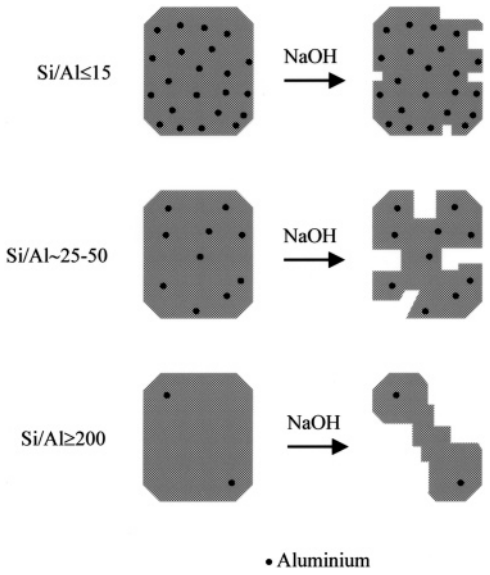

Figure 1. Simplified schematic representation of the influence of the Al content on the desilication treatment of MFI zeolites in NaOH solution and the associated mechanism of pore formation. Reprinted with permission from ref 100. Copyright 2004 American Chemical Society.

treatment, which preferentially removes framework Al atoms, alkali treatment was found to selectively extract framework Si atoms.[96,99−104] It was also shown that mesopore formation is preferentially initiated at boundaries or defect sites of the zeolite crystals.[95,100,103] Using N_2 adsorption, Groen et al. showed that the mesopores are not uniform but have a broad pore size distribution around 10 nm.[98] As a consequence of the introduction of mesoporosity, the external surface area increases from 40 to 130 $m^2\ g^{-1}$ in the treated samples; this increase comes at the expense of microporosity the volume of which decreases from 0.17 to 0.13 $cm^3\ g^{-1}$.[98] These authors subsequently identified the role of aluminum on the desilication process as well as described the mechanism of pore formation in MFT zeolites.[100] In the MFI framework, Si/Al < 20, the presence of high Al concentrations prevents Si from being extracted, thereby limiting pore formation. However, highly siliceous zeolites, Si/Al ≫ 50, show excessive and unselective Si dissolution, which leads to creation of relatively large pores. A framework Si/Al ratio of 25−50 is concluded to be optimal for substantial development of intracrystalline mesoporosity combined with preserved Al centers. The influence of the zeolite framework Si/Al ratio on Si extraction and the mechanism of porosity development are shown schematically in Figure 1. As a result of the negatively charged AlO_4^- tetrahedron, hydrolysis of the Si−O−Al bond in the presence of OH^- is hindered compared to the relatively easy cleavage of the Si−O−Si bond in the absence of neighboring Al tetrahedra. With application of scanning electron microscopy in combination with energy-dispersive X-ray analysis (SEM-EDX) and an advanced stereo-transmission electron microscopy (TEM) technique, it was further elucidated that because of the low concentration of Al in the interior of the crystals, Al gradients in ZSM-5 crystals induce the formation of hollow zeolite architectures with a well-preserved Al-rich exterior.[101] FT-IR measurements and NH_3 temperature programmed desorption (TPD) results confirm that an optimal alkaline treatment preserves the Al environment and the related acidic properties. The FT-IR absorption band at 3610 cm^{-1}, typical of Brønsted acid sites, disappeared after alkaline treatment but

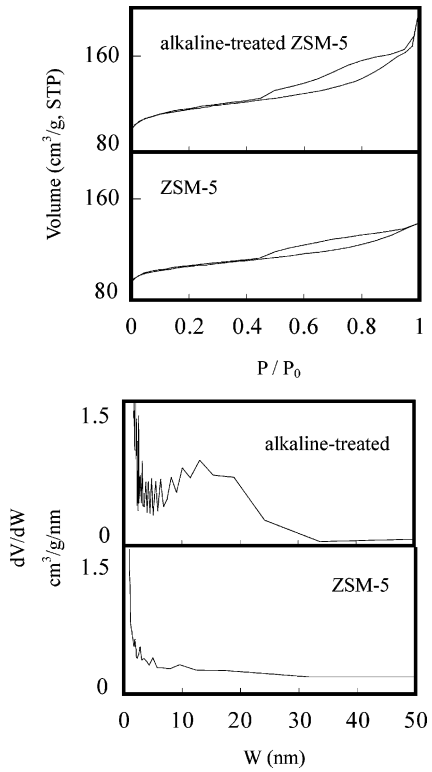

Figure 2. N_2 adsorption isotherms at 77 K for ZSM-5 with a SiO_2/Al_2O_3 molar ratio of 24 and the alkaline-treated ZSM-5 (the upper) and their BJH adsorption pore size distributions (lower panel).

was fully restored upon ion exchange in NH_4NO_3 and subsequent calcination.[100] A complementary investigation by Su et al. using solid-state NMR showed that the dissolution of the zeolite framework begins at the framework Si−O−Si linkages. The inertness of the Si−O−Al bond toward alkali treatment preserves the Brønsted acid sites (bridging OH species on Si−O−Al linkages).[103]

Changes in structural properties of ZSM-5 zeolites were studied using different SiO_2/Al_2O_3 molar ratios under mild conditions with low concentration NaOH solutions.[105] Characterization of the resulting ZSM-5 zeolites by low-temperature nitrogen and argon adsorption showed that the changes in structural properties depend on the SiO_2/Al_2O_3 molar ratios. Alkaline treatment of low SiO_2/Al_2O_3 ratio, 24, ZSM-5 yielded mesopores with a broad size distribution (Figure 2). Alkaline treatment of high SiO_2/Al_2O_3, 200, ZSM-5 did not show evidence of mesopores by adsorption.

3.2. Hydrothermal and Chemical Treatments

Numerous papers have been published on hydrothermal and chemical treatment of zeolites and effects on their structures, as well as their Brønsted and Lewis acid sites. Generally, postsynthesis hydrothermal dealumination treatment has been used to produce 5−50 nm defect domains in faujasites, mainly zeolite Y.[82,106−112] Combined high-resolution electron microscopy, scanning transmission electron microscopy, and energy-dispersive X-ray spectroscopy investigations showed that the mesopores in most of the USY grains are inhomogeneously distributed.[111] Some grains appear to contain more mesopores than others, and cracks have evolved in regions with high mesopore concentration. These domains have lost much of their crystallinity, resulting in a decreased amount of the active phase. By dealumination

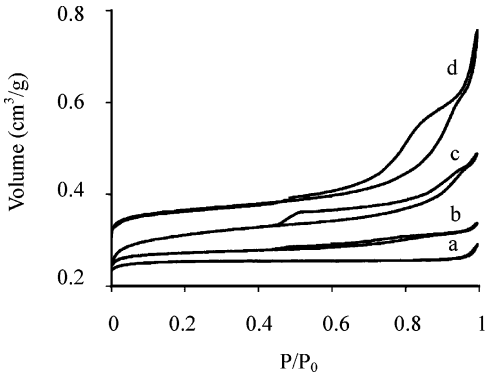

Figure 3. Adsorption isotherms of nitrogen at 77 K on several Y zeolites: (a) NaY (CBV100); (b) USY (CBV400, steamed once); (c) XVUSY (CBV780, steamed twice and acid leached); (d) HMVUSY (high-meso very ultrastable Y). For clarity the isotherm of NaY has been shifted 0.08 mL/g downward and the isotherm of the HMVUSY has been shifted upward by 0.15 mL/g. Reprinted with permission from ref 116. Copyright 2002 American Chemical Society.

of zeolite Y with steam at high temperature, Sasaki et al. showed that mesopores formed along the [110] directions in the preexisting [111] twin planes.[112,113] Using mercury porosimetry and hexane adsorption measurements, Lohse et al. showed that a 10 nm mesopore system is formed upon steaming of zeolite Y, and after extraction of extraframework material with an acid, the pore diameter increased to 20 nm.[114] Steam treatment of zeolite Y produced mesopores, 4−20 nm in diameter, amounting to a volume fraction of 20%.[115] After more severe steaming, followed by acid leaching, the volume fraction increased to 29%. Janssen et al. investigated the shape of the mesopores in Y zeolites modified by different postsynthesis treatments.[116,117] Using a combination of three-dimensional transmission electron microscopy, nitrogen adsorption, and mercury porosimetry, they showed that mild hydrothermal and acid leaching treatments result in many cavities within the crystals, while more severe treatments cause a loss of crystallinity and a decrease of micropore volume.[116,117] Very often, treatments produce deposits of material inside the micro- and mesopores, leading to partial blockage of the active sites. The nitrogen adsorption and desorption isotherms, shown in Figure 3, clearly show that the adsorption amounts, as well as the shapes of the hysteresis loops, $P/P_0 = 0.4$ to ~ 1, are very different owing to the different postsynthesis treatments of zeolite Y.[116] It is clear that hydrothermal treatment of zeolites cannot provide uniformly sized mesopores with well-defined lattice positions. Such inhomogenities are even more pronounced for higher temperature, steam-treated commercial USY cracking catalysts.[82,111,112] Hydrothermal treatment of other zeolites such as mazzite,[118,119] mordenite,[19,120,121] and ZSM-5[16,122,123] also have been reported.

Extraction of aluminum from higher aluminum-containing zeolites, such as UFA and LTA, by treatment with ammonium hexafluorosilicate (AFS),[124,125] ethylenediaminetetraacetic acid,[126,127] and $SiCl_4$[128−130] also has been reported. López-Fonseca et al. characterized the textural properties of a series of Y zeolites dealuminated by AFS and observed, via N_2 adsorption, a small amount mesopores were formed.[124] However, for zeolite Y with severe dealuminization, they observed the formation of mesopores along with considerable structural degradation resulting in a significant loss of micropore volume.[124] When zeolite Y was dealuminated by $SiCl_4$, little mesoporosity was generated and most of the microporosity of the zeolite was preserved.[131] Le Van Mao et al. showed that the textural and adsorptive properties of Ca-A zeolite undergo significant changes upon mild leaching, controlled hydrothermal treatment, or chemical treatment with AFS.[132] Aqueous AFS solution, under mild conditions (e.g., room temperature, pH $\approx$ 7.0), created slit-shaped mesopores with a distribution maximum at 14−20 nm; the average pore diameter depends on the rate of addition of the AFS solution to the leaching medium. The Si/Al ratio was observed to increase using AFS treatment, but not very dramatically, and the Al atoms retain their tetrahedral configuration as shown by ^{27}Al solid-state NMR spectroscopy. If the AFS treatment is combined with acid leaching or hydrothermal treatment, the N_2 adsorption capacity is significantly increased by the removal of extraframework material.

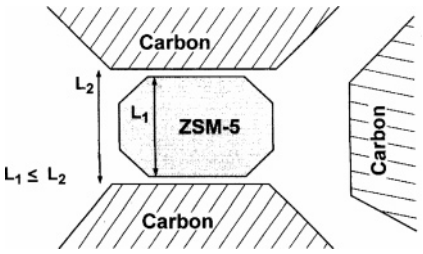

Figure 4. Confined space synthesis. The zeolite is crystallized within the pore system of a mesoporous carbon matrix. The crystal size, L_1, is always smaller than the pore diameter, L_2. Reprinted with permission from ref 139. Copyright 2000 American Chemical Society.

Dealumination of zeolites not only modifies the pore structures but also causes changes in Brønsted and Lewis acid sites.[119,126,133−135] Since zeolites have applications in the chemical and petrochemical industries as acid catalysts, knowledge of the active sites and their locations of the dealuminated zeolites is required for the design of efficient industrial catalysis. As noted above, the active centers of zeolites are Brønsted acid sites formed by bridging OH groups. On steaming, the aluminum removed from the framework remains in the cavities as nanoparticles whose surfaces possess Lewis acidity.[133−135] These Lewis sites may have their own catalytic activity or may interact with Brønsted sites, inducing an increase in acid strength and thus a modification of catalytic activity.[136−138] Nesterenko et al. characterized dealuminated mordenites (treated with methanesulfonic acid) by various techniques including X-ray diffraction, TPD-NH_3, N_2 adsorption, ^{1}H MAS NMR, and IR spectroscopy.[19] An increase in dealumination causes an increase of the Si/Al ratio and pore volumes, a decrease in the total amount of acid sites (including bridging and extraframework hydroxyls), an increase in the number of silanol groups, and an increase of Lewis acidity.

3.3. Nanosized Zeolites with Interparticle Mesopores

Nanospace considerations have provided an impetus to framework structural synthesis and modification. For example, nanosized zeolite ZSM-5 particles have been synthesized with mesoporosities. Jacobsen et al. reported confined space synthesis (see Figure 4) of several zeolites, which involved crystallization of the zeolite inside an inert mesoporous matrix.[21,22,139] Synthesized were ZSM-5 with Si/Al ratios of 50, 100, and ∞ (silicalite-1) with controlled average crystal sizes in the range 20−75 nm, nanosized

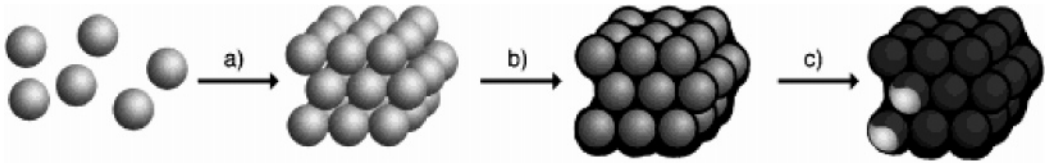

Figure 5. The synthesis of porous solids from rigid colloidal templates occurs in three steps: (a) assembly of colloidal particles into a regular array, (b) impregnation of template with monomer(s) and polymerization, and (c) removal of the template. Reprinted with permission from ref 142. Copyright 1999 Wiley-VCH.

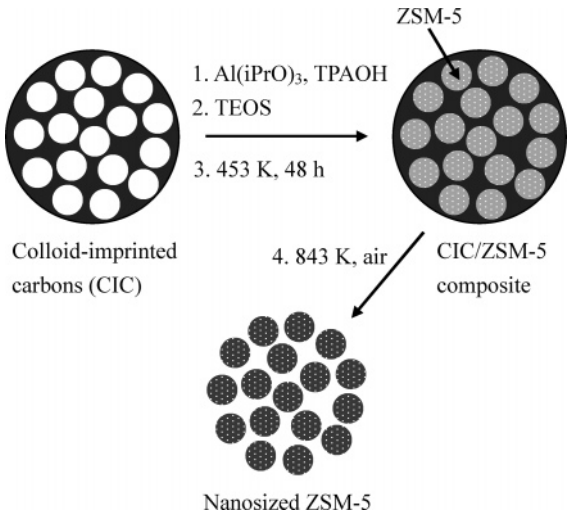

Figure 6. Scheme for the nanocasting synthesis of ZSM-5 zeolite. Reprinted with permission from ref 86. Copyright 2003 American Chemical Society.

zeolite β (7−30 nm), zeolite X (22−60 nm), and zeolite A (25−37 nm).[139] The synthesized material incorporating nanosized ZSM-5 had mesopores with a volume of 0.58 cm^3 g^{-1} and an average pore width of ∼35 nm, resulting from the packing of nanosized ZSM-5 crystals. The synthesis conditions influence the morphology of the zeolites. High nucleation rates favor formation of nanosized zeolites whereas low nucleation rates favor formation of mesoporous zeolites.[140] X-ray powder diffraction and nitrogen adsorption/desorption characterization indicate that nanosized ZSM-5 zeolites are highly crystalline. Jacobsen et al. studied the acidic properties of nanosized ZSM-5 prepared using confined nanospace synthesis by determination of relative numbers of Si*$(OSi)_4$, HOSi*$(OSi)_3$, and AlOSi*$(OSi)_3$ units with ^{27}Al and ^{29}Si magic-angle spinning (MAS) NMR spectroscopy and by ammonia desorption. Nanosized ZSM-5 crystals have a higher number of HOSi*$(OSi)_3$ sites but the same number of acid sites as much larger crystals when the Si/Al ratio is similar.[22] Because the acid sites and mesopore channels are important in catalysis, these mesostructural, nanosized zeolites may be used in heterogeneous catalytic processes.

Through the use of colloids as templates, colloid-imprinted carbons (CIS) have been prepared.[141] The principle of "direct templating" synthesis is shown schematically in Figure 5.[142] Kim et al. recently took nanocasting one step further (Figure 6). Through the use of CIS as the templating medium, they synthesized ZSM-5 zeolites with highly uniform particles.[86] The uniformity of the nanoparticles correlates with the uniformity of the pores in the initial imprinted carbon template. Nanocasting of ZSM-5 zeolite was accomplished by impregnating the CIS pores with a mixture of zeolite precursors and digestion of the composite mixture under hydrothermal conditions. Due to the size and shape fidelity of nanocasting, all of the zeolite phase in the nanodomain form had a morphology that corresponded to the pores in the carbon template. Nitrogen adsorption/desorption isotherms for the ZSM-5 nanoparticles exhibited steep uptakes at low relative pressures and hysteresis loops extending from $P/P_0 \approx 0.8-1$, suggesting the coexistence of micropores and mesopores. Via a rational choice of template pore size, the external surface area (16−127 cm^2 g^{-1}) and the interparticle mesopore volume (0.05−1.19 cm^3 g^{-1}) of CIS-nanocasted zeolite may be controlled.

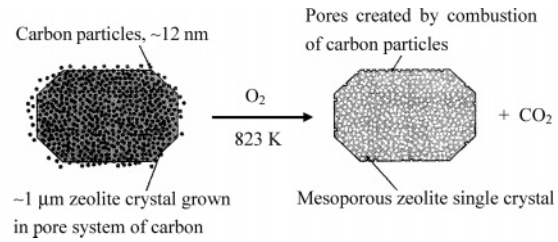

Figure 7. Growth of zeolite crystals around carbon particles. The zeolite is nucleated between the carbon particles; the pores are sufficiently large, and the gel is sufficiently concentrated to allow growth to continue within the pore system. Reprinted with permission from ref 83. Copyright 2000 American Chemical Society.

3.4. Template Methods

3.4.1. Carbon Black (CB), Multiwall Carbon Nanotube (MWNT), and Carbon Nanofiber (CNF) Templating

Although various strategies have been proposed to design zeolites with mesopores, template-directed synthesis is currently the most widely used method because of its versatility. By using an excess of gel, Jacobsen et al. grew zeolites on carbon particles embedded within the pore system of an inert matrix followed by burning off of the carbon matrix; the synthesis scheme is shown as Figure 7.[83] They prepared large zeolite ZSM-5 crystals with a pore distribution of 10−100 nm. Since some of the pores are larger than 50 nm, they belong to the class of IUPAC macropores,[143] and strictly speaking, this method should be called "macro-templating". By similar routes, mesoporous titanium silicalite-1, titanosilicalite-2, silicalite-2, and ZSM-11 zeolites were also synthesized.[84,144] The nitrogen adsorption and desorption isotherms of those zeolites, shown in Figure 8, have different hysteresis loops at high relative pressures, P/P_0 = ∼0.8−1, and different uptakes of N_2 at low relative pressures. These results show how the micro- and mesoporosities of the synthesized mesoporous zeolites can be varied by using different sized carbon black particles as inert matrixes. Holland et al., using monodisperse polystyrene spheres, synthesized macroporous silicates composed of silicalite walls with ∼50% crystallinity, ∼0.1 cm^3 g^{-1} micropore volume, and macropores of 250 nm average diameter.[85]

Jacobsen et al. also investigated using multiwall carbon nanotubes (MWNTs) as mesopore-forming templates.[87,88]

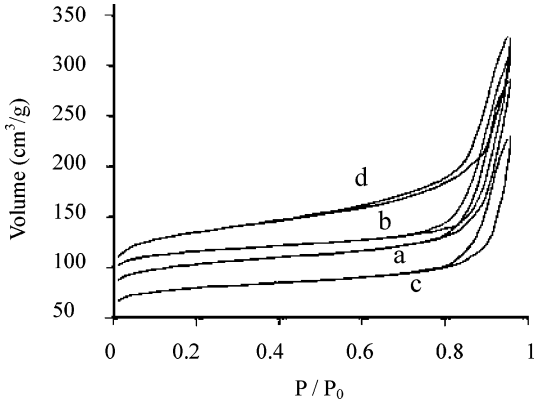

Figure 8. N_2 adsorption/desorption isotherms of mesoporous MEL-type zeolites templated with carbon particles: (a) silicalite-2 synthesized with BP-2000; (b) Na−ZSM-11 synthesized with BP-2000; (c) TS-2 synthesized with BP-2000; (d) TS-2 synthsized with BP-700. Reprinted from ref 84 with permission of Springer Science and Business Media, copyright 2004.

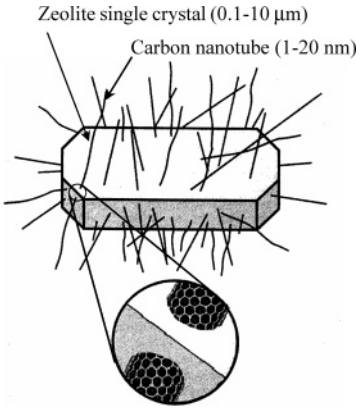

Figure 9. Schematic illustration of the synthesis principle for crystallization of mesoporous zeolite single crystals. Reprinted with permission from ref 87. Copyright 2001 American Chemical Society.

Taking the synthesis costs into account, carbon nanofibers (CNFs) were employed as templates for preparation of mesoporous zeolite single crystals since they can be produced much more cheaply than carbon nanotubes.[145,146] When MWNTs are used as the mesopore-forming template, individual zeolite crystals partially encapsulate the nanotubes during growth; this synthesis method is shown schematically in Figure 9. Selective removal of the nanotubes by combustion leads to formation of intracrystalline mesopores. By this route, highly crystalline zeolite crystals 100−500 nm in size can be prepared that contain uniform and straight mesopores of 12−30 nm widths, corresponding to the diameters of the carbon nanotubes. The amount of mesopores in the zeolite crystals is determined by the ratio of carbon nanotubes to zeolite gel.[88] The use of MWNTs as templates offers a high degree of control over the diameters and spatial arrangement of mesopores in zeolite crystals. Additionally, the zeolites contained iron oxide particles, <5 wt %, which had originally been encapsulated as impurities in the carbon materials.[88] Using CNFs as templating agents yields zeolite crystals whose mesopores vary widely in diameter. Some particles have pore diameters equal to the diameters of single CNFs, 20−40 nm, while others have much larger diameters. As shown in Figure 9, templating with either CNTs or CNFs causes the interconnected mesopores to begin at the external surface and run through the zeolite crystals.

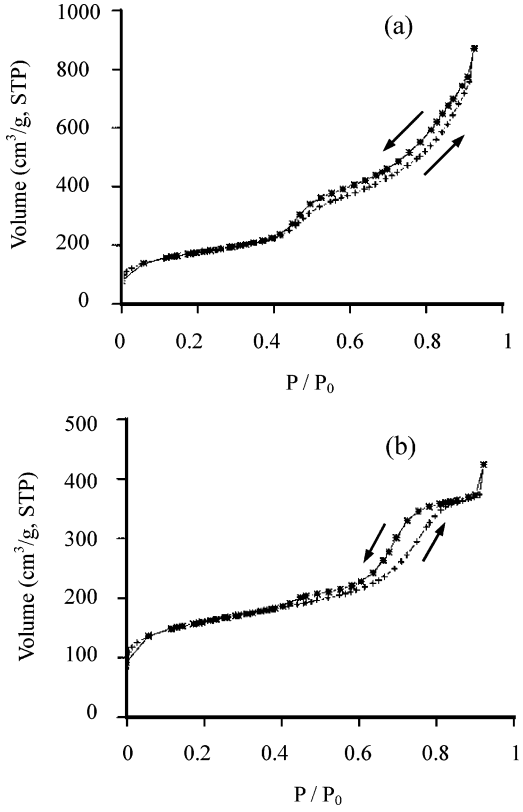

Figure 10. N_2 adsorption/desorption isotherms of RMMs: (a) from CMK-1 templating and (b) from CMK-3 templating. The hysteresis loops above $P/P_0 = 0.45$ (a) and 0.65 (b) are characteristic of capillary condensation in mesoporous channels. Reprinted with permission from ref 147. Copyright 2004 American Chemical Society.

3.4.2. Carbon Mesoporous Molecular Sieve (CMK) Templating

About the same time, Sakthivel et al.[147] and Yang et al.[148] reported templating by using carbon mesoporous molecular sieves (CMKs). Sakthivel et al. replicated mesoporous aluminosilicate molecular sieves, RMMs, using CMKs. Attempts to prepare RMMs from CMK by using a nanosized precursor of ZSM-5 resulted in formation of zeolite nanocrystals on the external surface of the carbon template. RMMs were synthesized by first treating the mesoporous carbon with tetrapropylammonium hydroxide (TPAOH) and then introducing aluminosilicates, followed by crystallization. Materials prepared by CMK-1 and CMK-3 templating possessed uniform pores with cubic and hexagonal patterns. By means of XRD, SEM, FT-IR, and ^{27}Al MAS NMR characterization, they were shown to be less ordered and with reduced crystallinity compared to conventional ZSM-5.[147] Nitrogen adsorption/desorption isotherms at 77 K, Figure 10, show a total pore volume of 0.8−0.9 $cm^3\ g^{-1}$, which is typical for a mesoporous structure. But, the micropore BET surface area, ≤178 $cm^2\ g^{-1}$, and volume, ≤0.08 $cm^3\ g^{-1}$, are much smaller than that of a highly crystalline ZSM-5 zeolite[147] indicating the presence of a lower-crystallinity preparation.[149] In contrast, Yang et al. prepared a highly crystallized ZSM-5 zeolite using CMK-3 as a template.[148] It appears, not too surprisingly for the synthesis of zeolites, that the precise conditions and starting materials account for the difference in preparations. We note that the Sakthivel group prepared the materials by introducing aluminosilicates in the confined space of CMKs and that the excess amount

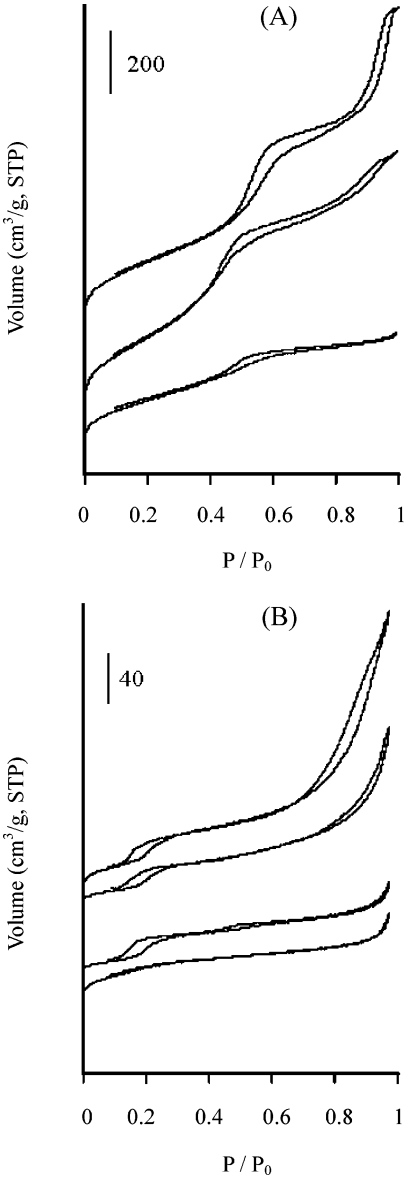

Figure 11. N_2 adsorption isotherms of (A) CMKs and (B) ZSM-5 zeolites from corresponding CMK templating (that of a conventional ZSM-5 is included at the bottom for comparison). Reprinted with permission from ref 148. Copyright 2004 Wiley-VCH.

of TPAOH was filtered and washed by distilled water then by ethanol before crystallization to prevent formation of zeolite nanocrystals on the external surface of the carbon template. Yang's group prepared a mixture of CMK and impregnated synthesis gel, and the resulting mixture was heated in an autoclave to crystallize the ZSM-5 zeolite; washing was not reported. The absence of washing could lead to formation of zeolite nanocrystals on the external surface of the CMK template or in the nanospace of CMK aggregates, resulting in larger mesopores indicated by the hysteresis loops at P/P_0 above ~0.8 in the 77 K nitrogen adsorption/desorption isotherms (Figure 11).[148] The hysteresis loops at P/P_0 above 0.8 are associated with the presence of large mesopores arising from textural mesoporosity. However the hysteresis loop at $P/P_0 \approx 0.2$ cannot be attributed to pore filling into supermicropores or small mesopores. Hysteresis loops at $P/P_0 \approx 0.2$ in nitrogen isotherms of some ZSM-5 samples have been previously reported for certain samples of silicalite-I by Carrott and Sing.[150]

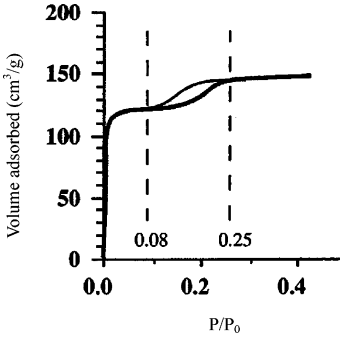

Figure 12. Nitrogen adsorption/desorption isotherms of ZSM-5 (Si/Al ≈ 50) at 77 K. Reprinted from ref 151, Copyright 1994, with permission from Elsevier.

On the basis of the fact that an increase in the volume of adsorption of nitrogen at 77 K occurs at a relative pressure of ~0.18 for ZSM-5 zeolite (Figure 12), Bonardet et al. studied the nature of nitrogen below and above this relative pressure by in situ ^{15}N NMR.[151] Two states (phases) of nitrogen were evident, but a solid phase of nitrogen was not evident even though the temperature was decreased to below 11 K at a relative pressure of 0.25. By means of Tian−Calvet isothermal microcalorimetry and neutron diffraction techniques, an energetic and structural study further confirmed that the low-pressure hysteresis and associated energy changes are due to a phase transition in the nitrogen adsorbate.[152−154] The formation of a more restricted adsorbed phase first occurs within the smaller dimensions of the void network followed by formation of the second phase within the larger void spaces. Therefore, different packing densities of adsorbed nitrogen in ZSM-5 zeolite causes the two plateaus, which are dependent on the relative pressure P/P_0, in the nitrogen isotherms. Kyriakou et al. made a systematic study of the nature of the low-pressure hysteresis loop observed in the nitrogen adsorption isotherms of some MFI zeolites with different counterions (specifically NH_4^+, Ca^{2+}, and Cu^{2+}).[155] They found from diffuse reflectance infrared Fourier transform (DRIFTS) spectra that the differences in the structural OH groups present, not associated with molecular water, are due to their association with the counterions. The position of the low-pressure hysteresis loop is influenced by the presence of defects in the crystals. Adsorption in a tubular channel system such as that of an MFI zeolite proceeds in two steps.[156] First, localized adsorption occurs at preferential high-energy sites, and second, clustering then occurs around the adsorbed molecules. Depending on ZSM-5 zeolite crystal size, aluminum content, and the presence of defects, the formation of a more restricted nitrogen phase causes the observed hysteresis loop at $P/P_0 \approx 0.2$.

3.4.3. Carbon Aerogel Templating

Carbon aerogels, CAs, are a version of the resorcinol−formaldehyde, RF, aerogel that is pyrolized in an inert atmosphere such as nitrogen (discussed in the following section).[157−163] CAs are obtained in a monolithic form and their structures and properties depend on the agglomerate structures of uniform spherical carbon particles.[162,164] Adsorption and desorption isotherms of N_2 on typical CAs at 77 K show IV type isotherms and clear hysteresis loops of type H1, suggesting that CAs are predominantly mesoporous (Figure 13).[165] CAs have uniquely different properties compared to uncarbonized organic aerogels, and they are

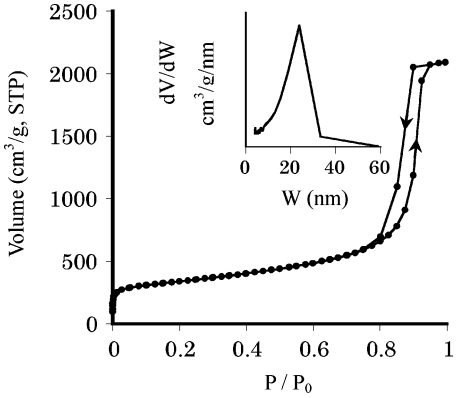

Figure 13. Adsorption/desorption isotherms of nitrogen at 77 K on CAs. Inset shows DH (Dollimore Head method) mesopore size distribution of CAs. Reprinted with permission from ref 165. Copyright 2003 Multi-Science.

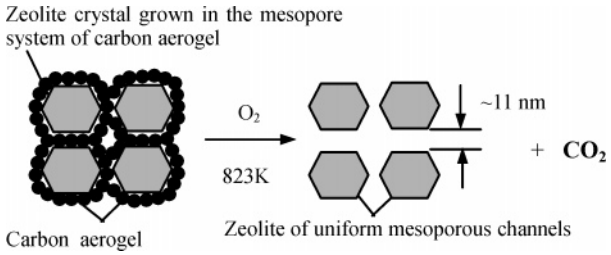

Figure 14. Growth of zeolite crystals in uniform mesopores of carbon aerogel consisting of interconnected uniform carbon particles. The mesopores are large enough to allow the gel to be sufficiently concentrated and to allow growth to continue until the mesopores are filled. Reprinted with permission from ref 89. Copyright 2003 American Chemical Society.

used for a wide variety of applications such as hydrogen fuel storage,[166] catalysis,[167] electric double layer capacitance,[168,169] and chromatographic separation. The preparation and properties of resorcinol−formaldhyde organic and carbon gels have recently been reviewed by Pierre et al.[170] and Al-Muhtaseb et al.[171]

Since the predominant pores in carbon aerogels are mesopores whose size can be controlled by using shrinkage of the RF aerogels during pyrolysis, a unique application of these materials has been developed as templates for the preparation of mesopore-modified zeolites.[89,90] The synthesis of mesopore-modified zeolites consists of three steps: (1) introducing the zeolite precursor into mesopores of carbon aerogel; (2) synthesizing zeolite in the inert mesopores of the carbon aerogel; (3) separating the zeolite crystals from the carbon aerogel.

Since zeolite crystals are intergrowths in the three-dimensional pore system of the CA monolith, complete combustion of the carbon material produces a mesopore-modified zeolite with large domain sizes. The principle of the synthesis scheme is shown schematically in Figure 14.[89]

By use of a CA with mesopore size of 23 nm and pore-wall thickness of ∼10 nm as a template, zeolites ZSM-5 and Y containing uniform mesopores have been synthesized. N_2 adsorption isotherms of both preparations not only show much larger adsorption amounts than the corresponding conventional zeolites but also display hysteresis loops in their N_2 isotherms above $P/P_0 = 0.6$ (Figures 15 and 16). The hysteresis loops at high relative pressure provide evidence for the presence of mesopores. The mesopore size distributions of these zeolites are narrow with maxima at ∼11 nm

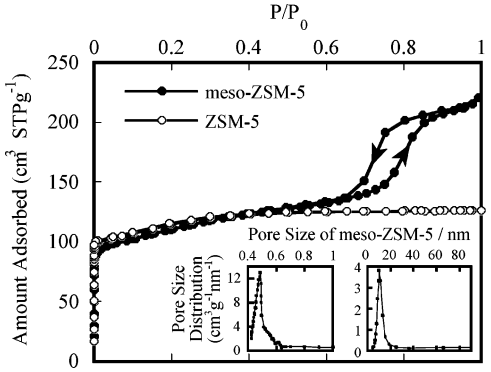

Figure 15. Adsorption/desorption isotherms of nitrogen at 77 K on ZSM-5 (○) and mesoporous ZSM-5 (●). Inserts show Saito−Foley micropore and DH mesopore size distributions of mesoporous ZSM-5. Reprinted with permission from ref 89. Copyright 2003 American Chemical Society.

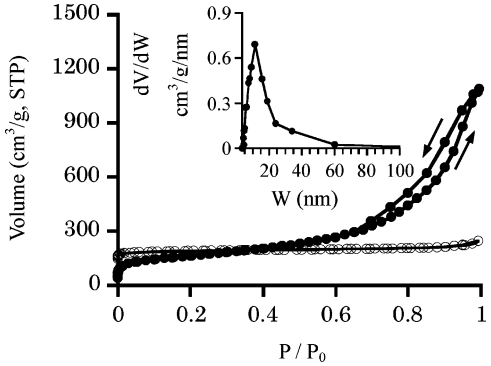

Figure 16. Adsorption/desorption isotherms of nitrogen at 77 K on mesoporous zeolite Y (●) and zeolite Y (○). Inset shows DH mesopore size distribution of mesoporous zeolite Y. Reprinted with permission from ref 90. Copyright 2003 American Chemical Society.

(see insets of Figures 15 and 16), which correspond to the wall thickness of the pores of the CA template, indicating rigid-structure casting. Hypothetically, by variation of the mesopore structures of the carbon aerogel template through solution chemistry, zeolites with controlled mesoporosity can been obtained. Characterization, using X-ray diffraction, FT-IR spectroscopy, and ^{29}Si nuclear magnetic resonance spectroscopy, indicates that the unit cell structures are the same as those for conventional zeolites; hence the mesopore-modified zeolites must have the same number of acid sites as conventional zeolites,[172] which depends on Al content in the framework of the zeolite.

3.4.4. Polymer Aerogel Templating

Resorcinol−formaldehyde, RF, aerogel, previously mentioned as a precursor of carbon aerogel, is a special type of low-density, open-cell foam derived from the polycondensation of resorcinol with formaldehyde.[157−159,173] The base-catalyzed, aqueous condensation of resorcinol (1,3-dihydroxy benzene) with formaldehyde forms a cross-linked and dark red gel. Variables, such as pH, reactant ratio, and temperature, influence the cross-linking chemistry and growth processes that take place prior to gelation. The size and number of resorcinol−formaldehyde clusters generated during the polymerization are controlled by the resorcinol/catalyst ratio in a formulation. Generally, drying of RF gels with supercritical CO_2 is then performed to remove liquid from the delicate gel structure without collapse or shrinkage.

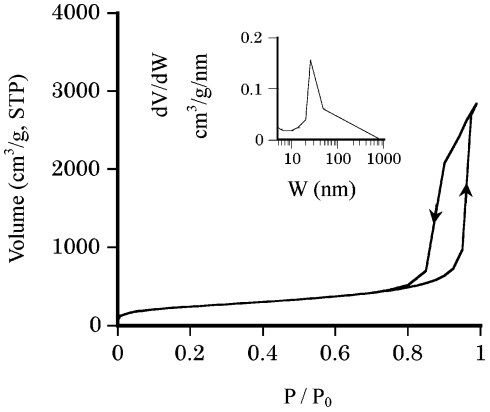

Figure 17. Adsorption and desorption isotherms of nitrogen at 77 K on RF aerogels. Insert shows the DH mesopore size distributions of RF aerogels. Reprinted with permission from ref 182. Copyright 2005 American Chemical Society.

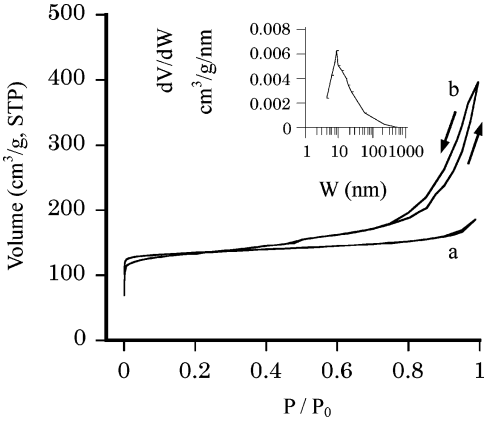

Figure 18. Adsorption and desorption isotherms of nitrogen at 77 K on zeolite A (a) and mesoporous zeolite A (b). Insert shows the DH mesopore size distributions of mesoporous zeolite A. Reprinted with permission from ref 182. Copyright 2005 American Chemical Society.

RF aerogels can be made using supercritical acetone.[174] Displacement of acetone by CO_2 is no longer necessary, so the process is shortened compared to drying with supercritical CO_2. This technique can be applied on a large scale for industrial purposes. Developed as an "ambient-pressure drying" process, it causes moderate shrinkage of the organic gel.[170] RF aerogels are easily produced in densities ranging from 0.035 to 0.100 g cm^{-3}. The RF aerogels are composed of interconnected beads of diameters smaller than 10 nm and cell sizes less than 100 nm in an open-celled structure with continuous porosity.[174] Since first synthesized by Pekala,[157−159,173] RF aerogels have received considerable attention in commercial applications such as adsorbents,[175] electrodes for capacitive deionization of aqueous solution,[176] ion-exchange resins,[177] electrochemical double layer capacitors and supercapacitors,[176] gas diffusion electrodes in proton exchange membrane (PEM) fuel cells,[178,179] and anodes in rechargeable lithium ion batteries.[180,181] Adsorption and desorption isotherms of N_2 at 77 K on representative RF aerogels are shown in Figure 17.[182] RF aerogels have a characteristic adsorption hysteresis, indicating that they are predominantly mesoporous with few micropores. Therefore, RF aerogels can provide mesostructures suitable for template synthesis.

As noted previously, highly crystalline mesopore-modified ZSM-5 and Y zeolites have been synthesized by using CA templating,[89,90] but it was not easy to synthesize mesopore-modified zeolite A.[182] It was recently reported that zeolite A with mesoporous channels was able to be synthesized using RF aerogels as templates due to their structural flexibility.[182] Characterization of the mesoporous zeolite A by powder X-ray diffraction, FT-IR spectra, and Raman spectroscopy reveals the structural characteristics of the Linde Type A framework without crystalline defects. The N_2 adsorption isotherm of the mesopore-modified zeolite A is IUPAC type IV, different from that of conventional zeolite A, which is a type I isotherm (Figure 18). The isotherm indicates the presence of mesopores, which were formed as a result of RF aerogel templating. Analysis of the adsorption isotherms using the Saito−Foley and the Dollimore and Heal (DH) methods revealed that the mesopore-modified zeolite A has a bimodal pore size distribution with micropores of ~0.4 nm and mesopores of 15 ± 5 nm; the total pore volume of the mesopore-modified zeolite A is 3 times that of conventional zeolite A.

Mesopore-modified ZSM-5 zeolites were prepared using RF aerogel templating with somewhat different mesoporosities compared with those from CA templating.[172] The mesopore volume is smaller and the pores are larger with a wider distribution via RF aerogel templating compared to the pore structure obtained from CA templating. The sizes and volumes of the mesoporous zeolites are closely related to the structures of the templates. Since CAs have relatively larger pore walls and less mesopore volume than RF aerogels, CAs can donate much larger mesopore volume to the mesoporous ZSM-5. The slightly thicker and nonuniform walls of RF aerogels result in larger mesopores with a broader distribution in the mesopore-modified ZSM-5.

The three-dimensional structure of the RF aerogel template depends on the size and number of clusters generated during the sol−gel polymerization, which, in turn, are determined by the resorcinol/catalyst ratio in a formulation. Therefore, solution chemistry can hypothetically be used to tune the structures of the RF aerogel template at the nanometer level. The organic frameworks are easily removed by burning under mild conditions (low temperature). The successful preparation and utilization of RF aerogels as templates will thus make it easier to design and synthesize mesoporous-modified zeolite crystals.

4. Applications

Zeolites have tridimensional networks of well-defined micropores. Although the molecular dimensions of the pores provide size or shape selectivity for guest molecules, it is known that because zeolites present a configurational regime of diffusion, the micropores restrict the diffusion rates of reactant and product, limiting the activity of zeolite catalysts for certain reactions.[13,183] On the other hand, the different diffusion rates of the reactants, products, or intermediates restricted or enhanced by pores are the basis for shape selectivity. Since diffusivity is proportional to pore diameter, addition of mesopores to zeolites can increase diffusion coefficients more than 2 orders of magnitude.[13] Moreover, from the stand point of large reactant molecules, the presence of mesopores in the zeolite will increase the external surface and pore openings accessible to the reactant.[1] By a combination of micro- and mesopores in dealuminated zeolite Y used for the cracking of vacuum gas oil, Corma found a

significantly higher conversion of molecules that are too large to penetrate into zeolite micropores.[1,184]

An approach was reported in which a layered MCM-22 material (the zeolite precursor of both MCM-22 and ERB-1 zeolites) is dealuminated in much the same way as the layered structure of a clay may be unbound.[185] The result is an aluminosilicate ITQ-2 (Insituto de Tecnología Quimíca) whose zeolite-type catalytic sites are contained within thin, readily accessible sheets. It was shown, by means of a cracking test using *n*-decane, that ITQ-2 catalyzed the formation of significantly more liquid and less gaseous product than the MWW-type zeolites. The reduced gas formation with ITQ-2 suggests that fewer consecutive reactions have taken place because the initial product molecules can diffuse rapidly out of the ITQ-2 framework. Hence the selectivity improvement can be attributed to the increased access to and from the catalytic sites for large molecules. Meima showed that the major factor determining the enhanced catalytic performance of dealuminated mordenites was the presence of mesopores.[121] One-dimensional mordenite micropores are interconnected by mesopores so that a two- or three-dimensional structure is obtained. Other factors, such as an enhanced acid strength of the remaining Brønsted sites, were also demonstrated.[115] van Donk et al. studied pore accessibility of zeolite mordenite and dealuminated mordenite (via a mild oxalic acid treatment) by using adsorption and diffusion measurements in combination with scanning electron microscopy/energy-dispersive X-ray (SEM/EDX) analysis. The results of transient uptake measurements for *n*-hexane in a tapered-element oscillating microbalance show the amount of *n*-hexane adsorbed in micropores almost tripled for the dealuminated zeolites.[186] With use of the tapered-element oscillating microbalance, the uptake experiments can be performed under full catalytic conditions.[14]

Alkylation of benzene with ethylene is a major industrial process responsible for production of almost all ethylbenzene (roughly 22×10^6 t/year[187]), which in turn is the raw material for styrene manufacture. Under reaction conditions close to those practiced commercially, mesoporous zeolite single crystals showed significantly improved catalytic activities and selectivities as compared to conventional zeolite.[188] The selectivity for ethylbenzene increases by 5−10% depending on the benzene conversion. The higher selectivities in the production of ethylbenzene using mesoporous zeolite catalyst were interpreted to be caused by improved mass transport in zeolite crystals. Whenever a benzene molecule is ethylated, it can either be transported into the product stream or undergo further ethylation; the shorter diffusion path suppressed further ethylation. Hence, by modifying mass transport, it is possible to obtain both higher activity and higher product selectivity using mesoporous zeolite catalysts.

For slurry-phase reactions where diffusion is much slower than for gas-phase reactions, the beneficial effect of mesopores should be even more pronounced. Indeed, mesoporous zeolite single crystals were found to exhibit pronounced activity enhancement over conventional zeolite catalysts in slurry-phase catalytic cracking and isomerization of *n*-hexadecane.[84,189] Enhanced cumene cracking was obtained using mesoporous ZSM-5 (subjected to an alkali treatment).[95] As expected, the mesoporous channels in ZSM-5 zeolites serve to enhance molecular diffusion of aromatic molecules, while micropores are the active sites for the formation of aromatics. Mo-modified catalysts prepared from the alkali-treated zeolites showed higher selectivity for aromatics and higher tolerance against carbonaceous deposits, thus leading to a very high catalytic performance in the conversion of methane to aromatics when compared with a conventional Mo/HZSM-5 catalyst.[103] Similarly, mesoporous TS-1 (templated using carbon black particles) catalyst was shown to be active in the epoxidation of oct-1-ene and was significantly more active in epoxidation of cyclohexene than conventional TS-1.[144] Mesoporous TS-2 (templated using carbon black particles) catalyst showed good performance in the epoxidation of oct-1-ene and styrene with regards to selectivity in comparison with conventional microporous catalysts.[84]

For a number of industrial catalytic applications such as catalytic cracking, hydrocracking, aromatic alkylation, and alkane hydroisomerization, as well as fine chemical synthesis, it has been demonstrated that the presence of mesopores in zeolite crystals alleviates diffusional limitations.[14,190−193] Mesoporous zeolites are being scouted for other processes of the refining industry such as *n*-paraffin isomerization, olefin oligomerization, olefin disproportionation, and the cracking of polyethylene and polypropylene.[131,194,195] Excellent overviews of the use of mesoporous zeolites have been reported.[1,115,196]

For environmental catalysis, Pérez-Ramírez et al. reported that the improved catalyst accessibility by the formation of mesopores upon alkaline posttreatment led to higher N_2O decomposition activities.[16] The experimental results that the NO*x* conversion over the Co/MFI-type zeolite through structural transformation of CTA^+−MCM-41 was much higher than that over a conventional Co/ZSM-5 catalyst support that presence of larger pores in the zeolites is helpful for the mass transfer of reactants and reaction products across the pores.[78] From the point that the zeolites with additional larger pores were similar to small crystals of Co/ZSM-5, which were reported to be more active than larger ones for selective catalytic reduction (SCR) of NO*x* by propane, the fast mass transfer diffusion has a positive influence on the activities of the catalyst.[197]

The increased external surface provided by mesoporous modification of zeolites not only decreases transport limitations but is also beneficial in achieving high dispersion of a catalytic phase. An example, recently reported, is that, after calcination, a metal (Pt), an alloy (PtSn), and a metal carbide (β-Mo_2C) were evenly distributed throughout the entire mesopore system of a zeolite support as nanocrystals.[198] This cannot be achieved with conventional zeolites because the supported catalysts aggregate on the outer surface of the zeolite particles during thermal treament. High loadings of nanocrystals can be obtained because the extensive pore system of mesoporous zeolites absorbs substantial amounts of precursor solutions. The highly dispersed nanocrystals are in close proximity to the active sites in micropores that are responsible for shape selectivity. Therefore, these materials, by combining the acidity of the zeolites with the catalytic properties of the supported component, are suitable candidates for bifunctional catalysis.[187,199,200] Access to the nanocrystal catalysts is possible through both the micropores and the mesopores. Incorporation of a high degree of mesoporosity in zeolite particles provides new opportunities for them as hosts for enclosure of other chemical entities.

The above-mentioned examples show that zeolites with mesopores have already exhibited promising properties in catalytic processes. We have no doubt that mesopore-added zeolites have opened new fields for future exploration.

Table 1. Summary of the Preparation Routes and Pore Structural Parameters of Mesoporous Zeolites[a]

mesoporous zeolites (synthesis method)	S_{BET} ($cm^2\ g^{-1}$)	S_{ext} ($cm^2\ g^{-1}$)	V_{total} ($cm^3\ g^{-1}$)	V_{micro} ($cm^3\ g^{-1}$)	W_{meso} (nm)	crystallinity	ref
ZSM-5 (posttreatment)	450	130	0.59	0.13	B	N	98
	320	N	0.412	0.133	~4[d]	high	94
	510	235	0.61[b]	0.13	~9	N	100
	328	63[c]	0.26	0.12	3−5	high	103
	377	204[c]	0.51	0.08	3−10	low	103
XVUSY (posttreatment)	N	120	0.53[b]	0.28	4−40	high	120
HMVUSY (posttreatment)	N	146	0.62[b]	0.15	4−25	high	120
mordenite (posttreatment)	N	N	~0.24	0.14−0.18	N	N	19
ZSM-5 (confined space)	412−434	185−251	0.64−1.06[b]	0.09−0.12	~35	high	21, 139
β (confined space)	651	168	2.67[b]	0.25	>100	high	139
ZSM-5 (CB templating)	N	N	1.10	0.09	10−100	high	83
ZSM-11 (CB templating)	397	N	0.53[b]	0.13	N	high	84
silicalite-2 (CB templating)	347	N	0.49[b]	0.10	N	high	84
TS-1 (CB templating)	N	N	~1.10	~0.09	~20	high	144
TS-2 (CB templating)	477	N	0.57[b]	0.13	N	high	84
	253	N	0.38[b]	0.07	N	low	84
ZSM-5 (MWNT templating)	~360	~120	N	N	12−30	high	88
Silicate-1 (CNF templating)	N	72	0.37	0.11	≥20−40	high	145
ZSM-5 (CMK1 templating)	554	400[c]	0.77	0.07	3−5	low	147
ZSM-5 (CMK3 templating)	594	417[c]	0.92	0.08	4−6	low	147
	281−382	132−234[c]	0.26−0.47	0.08−0.1	N[e]	high	148
ZSM-5 (CIS templating)	250−310	173−277	0.3−1.27	0.08−0.14	N	high	86
ZSM-5 (CA templating)	385	N	0.35	0.15	11 ± 2	high	89
	395	N	0.31	0.16	9 ± 1.5	high	172
ZSM-5 (RF templating)	427	N	0.25	0.18	9−25	high	172
	414	N	0.27	0.17	14 ± 3	high	172
NaY (CA templating)	581	N	1.58	0.21	10	high	90
NaA (RF templating)	472	N	0.63	0.20	15 ± 5	high	182

[a] N indicates that data are not given explicitly; B indicates that mesopore size distributions are broad. [b] $V_{micro} + V_{meso}$. [c] $S_{BET} - S_{micro}$. [d] Misinterpreted mesopore sizes from the N_2 desorption isotherm.[98] [e] It is not evidenced on supermicropores or small mesopores suggested in ref 148 based on hysteresis loops at $P/P_0 = \sim 0.2$ in N_2 adsorption and desorption isotherms.[150,151,153−156,205]

5. Future Scope

The success of the methods described above to create mesoporosity within zeolite crystals and particles will lead to additional efforts in this area. Other nanoporous polymers, such as melamine formaldehyde (MF) aerogels and diepoxy diamine, are available as template materials. MF aerogels are prepared from aqueous sol−gel polymerization of melamine with formaldehyde followed by supercritical drying with CO_2.[201] MF aerogels have low densities, high surface areas, continuous porosity, and ultrafine cell/pore size (<50 nm). Nanoporous polymers of diepoxy diamine are designed and prepared via reactive encapsulation of a chemically inert solvent of tetrahydrofuran (THF). Gels were synthesized by mixing stoichometric quantities of epoxy and amine (2:1 mole ratio, as each amine reacts with two epoxy groups) with varying amounts of solvent and subsequently followed by supercritical drying. By changing the solvent content, one can systematically tailor the pore sizes and volumes of the nanoporous materials synthesized by the reactive encapsulation technique up to 100 nm.[202]

It is apparent that the electrostatic interactions between the zeolite clusters and the polymer clusters of the template walls and favorable van der Waals contacts between zeolite nanoparticles provide the nanoparticles with enough mobility for the initial migration necessary for nucleation and crystallization within the template mesopores. Thus, this methodology should be able to be extended to other zeolites. Designed synthesis of crystalline zeolites with mesopores is a major challenge in the field of advanced materials.[2,203,204] The successful preparation and utilization of polymer aerogels as templates will provide flexible synthetic routes to a range of mesoporous zeolites and other nanoporous crystals.

6. Summary

This article presents a brief overview on the preparation and characterization of mesoporous zeolites and how the added mesoporosities are related to the synthesis and processing conditions. Mesopore-modified zeolites can be prepared via several routes as summarized in Table 1. Different posttreatments of the synthesized zeolites are used; alkaline leaching or hydrothermal and other chemical treatments are the most frequently applied. These treatments provide zeolites with an inhomogeneous distribution of mesopores formed from defect domains. Novel dual templating methods using carbon materials, which are removed by burning after synthesis, have recently been developed. Variations in mesostructures from carbon templating and hydrothermal synthesis conditions of zeolites provide significant variations in the structural characteristics of the resulting mesoporous zeolites. In many commercial applications, such as cracking of heavy oil fractions, cumene production, and alkane hydroisomerization, mesopore-modified zeolites are receiving considerable attention. The large variety of potential and existing commercial applications is largely due to the novel framework compositions of the mesopore-modified zeolites. It is anticipated that many new and exciting applications will arise due to the optimization of tunable mesoporous zeolite structures.

7. Acknowledgments

The authors thank the anonymous referees for helpful comments and suggestions that contributed to the improvement of this paper.

8. References

(1) Corma, A. *Chem. Rev.* **1997**, *97*, 2373.
(2) Davis, M. E. *Nature* **2002**, *417*, 813.
(3) Breck D. W. In *Zeolite molecular sieves*; Robert E. Krieger Publishing Company, Inc.: Malabar, FL, 1974.
(4) Ghose S.; Mattiasson B. *Biotechnol. Appl. Biochem.* **1993**, *18*, 311.
(5) Chen, N. Y.; Degnan, T. F. *Chem. Eng. Prog.* **1988**, *84*, 32.
(6) Pires, J.; Carvalho, A.; de Carvaho, M. B. *Microporous Mesoporous Mater.* **2001**, *43*, 277.
(7) Richter, M.; Berndt, H.; Eckelt, R.; Schneider, M.; Fricke, R. *Catal. Today* **1999**, *54*, 531.
(8) Zhang, W.; Smirniotis, P. G. *Appl. Catal. A* **1998**, *168*, 113.
(9) Kloetstra, K. R.; van Bekkum H.; Jansen J. C. *Chem. Commun.* **1997**, 2281.
(10) Yang, P.; Zhao, D.; Margolese, D.; Chmelka, B. F.; Stucky, G. D. *Nature* **1998**, *396*, 152.
(11) Yang, P.; Zhao, D.; Margolese, D.; Chmelka, B. F.; Stucky, G. D. *Chem. Mater.* **1999**, *11*, 2813.
(12) Smith, J. V. *Chem. Rev.* **1988**, *88*, 149.
(13) Kärger, J.; Ruthven, D. M. *Diffusion in Zeolites and Other Microporous Materials*; Wiley: New York, 1992.
(14) van Donk, S.; Broersma, A.; Gijzeman, O. L. J.; van Bokhoven, J. A.; Bitter, J. H.; de Jong, K. P. *J. Catal.* **2001**, *204*, 272.
(15) Herrmann, C.; Haas, J.; Fetting, F. *Appl. Catal.* **1987**, *35*, 299.
(16) Pérez-Ramírez, J.; Kapteijn, F.; Groen, J. C.; Domenech, A.; Mul, G.; Moulijn, J. A. *J. Catal.* **2003**, *214*, 33.
(17) Weisz, P. B.; *Chem. Technol.* **1973**, *3*, 498.
(18) Chen, N. Y.; Smith, C. M. *Molecular Transport and Reaction in Zeolite*; VCH: New York, 1994.
(19) Nesterenko, N. S.; Thibault-Starzyk, F.; Montouillout, V.; Yuschenko, V. V.; Fernandez, C.; Gilson, J.-P.; Fajula, F.; Ivanova, I. I. *Microporous Mesoporous Mater.* **2004**, *71*, 157.
(20) Lovallo, M. C.; Tsapatsis, M. In *Advanced Catalysts and Nanostructured Materials*; Moser, W. R., Ed.; Academic Press: San Diego, CA, 1996; Chapter 13.
(21) Madsen, C.; Jacobsen, C. J. H. *J. Chem. Soc., Chem. Commun.* **1999**, 673.
(22) Jacobsen, C. J. H.; Madsen, C.; Janssens, T. V. W.; Jakobsen, H. J.; Skibsted, J. *Microporous Mesoporous Mater.* **2000**, *39*, 393.
(23) Zhan, B. Z.; White, M. A.; Lumsden, M.; Jason, M. N.; Robertson, K. N.; Cameron, T. S.; Gharghouri, M. *Chem. Mater.* **2002**, *14*, 3636.
(24) Holmberg, B. A. W. H.; Norbeck, J. M.; Yan, Y. *Microporous Mesoporous Mater.* **2003**, *59*, 13.
(25) Li, Q.; Creaser, D.; Sterte, J. *Chem. Mater.* **2002**, *14*, 1319.
(26) Yamamura, M.; Chaki, K.; Wakatsuki, T.; Okado, H.; Fujimoto, K. *Zeolites* **1994**, *14*, 643.
(27) Mintova, S.; Bein, T. *Adv. Mater.* **2001**, *13*, 1880.
(28) Schwabb, E. A.; Gares, B. C. *Ind. Eng. Chem. Fundam.* **1972**, *11*, 540.
(29) Rajagopalan, K.; Peters, A. W.; Edwards, G. C. *Appl. Catal.* **1986**, *23*, 69.
(30) Haag, W. O.; Lago, R. M.; Weisz, P. B. *Faraday Discuss.* **1982**, *72*, 317.
(31) Voogd, P.; van Bekkum, H. *Appl. Catal.* **1990**, *59*, 311.
(32) Bellussi, G.; Pazzuconi, G.; Perego, C.; Girotti, G., Teroni, G. *J. Catal.* **1995**, *157*, 227.
(33) Camblor, M. A.; Corma, A.; Martínez, A.; Martínez-Soria, V.; Valencia, S. *J. Catal.* **1998**, *179*, 537.
(34) Camblor M. A.; Corma A.; Valencia S. *Microporous Mesoporous Mater.* **1998**, *25*, 59.
(35) Nhut J. M.; Pesant L.; Tessonnier J. P.; Wine G.; Guille J.; Cuong P. H.; Ledoux M. J. *Appl. Catal. A* **2003**, *254*, 345.
(36) Rajagopalan, K.; Peters, A. W.; Edwards, G. C. *Appl. Catal.* **1986**, *23*, 69.
(37) Camblor, M. A.; Corma, A.; Martínez, A.; Mocholí, F. A.; Pérez-Pariente, J.; *Appl. Catal. A* **1989**, *55*, 65.
(38) Kresge, C. T.; Leonowicz, M. E.; Roth, W. J.; Vartuli, J. C.; Beck, J. S. *Nature* **1992**, *359*, 710.
(39) Beck, J. S.; Vartuli, J. C.; Roth, W. J.; Leonowicz, M. E.; Kresge, C. T.; Schmitt, K. D.; Chu, C. T.-W.; Olson, D. H.; Sheppard, E. W.; McCullen, S. B.; Higgins, J. B.; Schlenker, J. L. *J. Am. Chem. Soc.* **1992**, *114*, 10834.
(40) Galarneau, A.; Barodawalla, A.; Pinnavaia, T. J. *Nature* **1995**, *374*, 529.
(41) Yanagisawa, T.; Shimizu T.; Kuroda K.; Kato C. *Bull. Chem. Soc. Jpn.* **1990**, *63*, 988.
(42) Inagaki, S.; Fukushima, Y.; Kuroda, K. *J. Chem. Soc., Chem. Commun.* **1993**, 680.
(43) Linssen, T.; Cassiers, K.; Cool, P.; Vansant, E. F. *Adv. Colloid Interface Sci.* **2003**, *103*, 121.
(44) Tanev, P. T.; Pinnavaia, T. J. *Science* **1995**, *267*, 865.
(45) Tanev, P. T.; Chibwe, M.; Pinnavaia, T. J. *Nature* **1994**, *368*, 321.
(46) Tanev, P. T.; Pinnavaia, T. J. *Chem. Mater.* **1996**, *8*, 2068.
(47) Bagshaw, S. A.; Prouzet, E.; Pinnavaia, T. J. *Science* **1995**, *269*, 1242.
(48) Blin, J. L.; Becue, A.; Pauwels, B.; Van Tendeloo, G.; Su, B. L. *Microporous Mesoporous Mater.* **2001**, *44*, 41.
(49) Boissiere, C.; Larbot, A.; van der Lee, A.; Kooyman, P. J.; Prouzet, E. *Chem. Mater.* **2000**, *12*, 2902.
(50) Blin, J. L.; Leonard, A., Su, B. L. *J. Phys. Chem. B* **2001**, *105*, 6070.
(51) Ryoo, R.; Kim, J. M.; Ko, C. H.; Shin, C. H. *J. Phys. Chem.* **1996**, *100*, 17718.
(52) Zhao, D.; Feng, J.; Huo, Q.; Melosh, N.; Fredrickson, G. H.; Chmelka, B. F.; Stucky, G. D. *Science* **1998**, *279*, 548.
(53) Zhao, D.; Huo, Q.; Feng, J.; Chmelka, B. F.; Stucky, G. D. *J. Am. Chem. Soc.* **1998**, *120*, 6024.
(54) Kim, J. M.; Stucky, G. D. *Chem. Commun.* **2001**, 1159.
(55) Cassiers, K.; Linssen, T.; Mathieu, M.; Benjelloun, M.; Schrijnemakers, K.; Van Der Voort, P.; Cool, P.; Vansant, E. F. *Chem. Mater.* **2002**, *14*, 2317.
(56) Davis, M. E. *Nature* **1993**, *364*, 391.
(57) Davis, M. E. *Catal. Today* **1994**, *19*, 1.
(58) Gusev, V. Y.; Feng, X.; Bu, Z.; Haller, G. L.; O'Brien, J. A. *J. Phys. Chem.* **1996**, *100*, 1985.
(59) Van Der Voort, P.; Baltes, M.; Vansant, E. F. *Catal. Today* **2001**, *68*, 121.
(60) Kawi, S.; Shen, S.-C. *Mater. Lett.* **2000**, *42*, 108.
(61) Jun, S.; Kim, J. M.; Ryoo, R.; Ahn, Y.-S.; Han, M.-K. *Microporous Mesoporous Mater.* **2000**, *41*, 119.
(62) Corma, A.; Martinez, A.; Martinez Soria, V.; Monton, J. B. *J. Catal.* **1995**, *153*, 25.
(63) Landau, M. V.; Vradman, L.; Herskowitz, M.; Koltypin, Y.; Gedanken, A. *J. Catal.* **2001**, *201*, 22.
(64) Klimova, T.; Calderon, M.; Ramirez, J. *Stud. Surf. Sci. Catal.* **2001**, *135*, 4280.
(65) Shanthi, K.; Sasi Rekha, N. R.; Moheswari, R.; Sivakumar, T. *Stud. Surf. Sci. Catal.* **2001**, *135*, 4296.
(66) Kloetstra, K. R.; Zandbergen, H. W.; Jansen, J. C.; van Bekkum, H. *Microporous Mater.* **1996**, *6*, 287.
(67) Cho, S., II.; Kwon, Y. K.; Park, S.-E.; Kim, G.-J. *Stud. Surf. Sci. Catal.* **2003**, *146*, 137.
(68) Liu, Y.; Zhang, W.; Pinnavaia, T. J. *Angew. Chem., Int. Ed.* **2001**, *40*, 1255.
(69) Liu, Y.; Zhang, W.; Pinnavaia, T. J. *J. Am. Chem. Soc.* **2000**, *122*, 8791.
(70) Huang, L.; Guo, W.; Deng, P.; Xue, Z.; Li, Q. *J. Phys. Chem. B* **2000**, *104*, 2817.
(71) Karlsson, A.; Stöker, M.; Schmidt, R. *Microporous Mesoporous Mater.* **1999**, *27*, 181.
(72) Karlsson, A.; Stöker, M.; Schäfer, K. *Stud. Surf. Sci. Catal.* **2000**, *129*, 99.
(73) Trong On, D.; Lutic, D.; Kaliaguine, S. *Microporous Mesoporous Mater.* **2001**, *44*−*45*, 435.
(74) Trong On, D.; Kaliaguine, S. *Angew. Chem., Int. Ed.* **2001**, *40*, 3248.
(75) Guo, W.; Xiong, C.; Huang, L.; Li, Q. *J. Mater. Chem.* **2001**, *11*, 1886.
(76) Guo, W.; Huang, L.; Deng, P.; Xue, Z.; Li, Q. *Microporous Mesoporous Mater.* **2001**, *427*, 44.
(77) Xia, Y.; Mokaya, R. *J. Mater. Chem.* **2004**, *14*, 863.
(78) Chen, X.; Kawi, S. *Chem. Commun.* **2001**, 1354.
(79) Hidrobo, A.; Retuert, J.; Araya, P.; Wolf, E. *J. Porous Mater.* **2003**, *10*, 231.
(80) Trong On, D.; Kaliaguine, S. *Angew. Chem., Int. Ed.* **2002**, *41*, 1036.
(81) Zhang, Z.; Han, Y.; Zhu, L.; Wang, R.; Yu, Y.; Qiu, S.; Zhao, D.; Xiao, F.-S. *Angew. Chem., Int. Ed.* **2001**, *40*, 1258.
(82) Lynch, J.; Raatz, F.; Dufresne, P. *Zeolites* **1987**, *7*, 333.
(83) Jacobsen, C. J. H.; Madsen, C.; Houzvicka, J.; Schmidt, I.; Carlsson, A. *J. Am. Chem. Soc.* **2000**, *122*, 7116.
(84) Kustova, M. Y.; Hasselriis, P.; Christensen, C. H. *Catal. Lett.* **2004**, *96*, 205.
(85) Holland, B. T.; Abrams, L.; Stein, A. *J. Am. Chem. Soc.* **1999**, *121*, 4308.
(86) Kim, S. S.; Shah, J.; Pinnavaia, T. J. *Chem. Mater.* **2003**, *15*, 1664.
(87) Schmidt, I.; Boisen, A.; Gustavsson, E.; Stahl, K,; Pehrson, S.; Dahl, S.; Carlsson, A.; Jacobsen, C. J. H. *Chem. Mater.* **2001**, *13*, 4416.
(88) Boisen, A.; Schmidt, I.; Carlsson, A.; Dahl, S.; Brorson, M.; Jacobsen, C. J. H. *Chem. Commun.* **2003**, 958.
(89) Tao, Y.; Kanoh, H.; Kaneko, K. *J. Am. Chem. Soc.* **2003**, *125*, 6044.
(90) Tao, Y.; Kanoh, H.; Kaneko, K. *J. Phys. Chem. B* **2003**, *107*, 10974.
(91) Davis, S. A.; Burkett, S. L.; Mendelson, N. H.; Mann. S. *Nature* **1997**, *385*, 420.
(92) Göltner, C. G. *Angew. Chem., Int. Ed.* **1999**, *38*, 3155.
(93) Schüth, F.; Schmidt, W. *Adv. Mater.* **2002**, *14*, 629.
(94) Ogura, M.; Shinomiya, S.; Tateno, J.; Nara, Y.; Kikuchi, E.; Matsukata, M. *Chem. Lett.* **2000**, 882.

(95) Ogura, M.; Shinomiya, S.; Tateno, J.; Nara, Y.; Nomura, M.; Kikuchi, E.; Matsukata, M. *Appl. Catal. A: Gen.* **2001**, *219*, 33.
(96) Ogura, M.; Kikuchi, E.; Matsukata, M. *Stud. Surf. Sci. Catal*. **2001**, *135*, 11.
(97) Suzuki, T.; Okuhara, T. *Microporous Mesoporous Mater*. **2001**, *43*, 83−89.
(98) Groen, J. C.; Pérez-Ramírez, J.; Peffer, L. A. A. *Chem. Lett.* **2002**, 94.
(99) Groen, J. C.; Peffer, L. A. A.; Pérez-Ramírez, J. *Microporous Mesoporous Mater.* **2003**, *60*, 1.
(100) Groen, J. C.; Jansen J. C.; Moulijn J. A.; Pérez-Ramírez, J. *J. Phys. Chem. B* **2004**, *108*, 13062.
(101) Groen, J. C.; Bach, T.; Ziese, U.; Paulaime-van Donk, A. M.; de Jong, K. P.; Moulijn, J. A.; Pérez-Ramírez, J. *J. Am. Chem. Soc.* **2005**, *127*, 10792.
(102) Groen, J. C.; Moulijn, J. A.; Pérez-Ramírez, J. *Microporous Mesoporous Mater.* **2005**, *87*, 153.
(103) Su, L.; Liu, L.; Zhuang, J.; Wang, H.; Li, Y.; Shen, W.; Xu, Y.; Bao, X. *Catal. Lett*. **2003**, *91*, 155.
(104) Dessau, R. M.; Valyocsik, E. W.; Goeke, N. H. *Zeolites* **1992**, *12*, 776.
(105) Tao, Y.; Kanoh, H.; Groen, J. C.; Kaneko, K. *Stud. Surf. Sci. Catal.*, in press.
(106) Patzelová, V.; Jaeger, N. I. *Zeolites* **1987**, *7*, 240.
(107) Lynch, J.; Raatz, F.; Delalande, Ch. *Stud. Surf. Sci. Catal.* **1988**, *39*, 547.
(108) Maher, P. K.; Hunter, F. D.; Scherzer, J.; *Adv. Chem. Ser*. **1971**, *101*, 266.
(109) Cartlidge, S.; Nissen, H. U.; Wessicken, R. *Zeolites* **1989**, *9*, 346.
(110) Corma, A.; Diaz-Cabanas, M. J.; Martinez-Triguero, J.; Rey. F.; Rius, J. *Nature* **2002**, *418*, 514.
(111) Choi-Feng, C.; Hall, J. B.; Huggins, B. J.; Begerlein, R. A. *J. Catal.* **1993**, *140*, 395.
(112) Sasaki, Y.; Suzuki, T.; Takamura, Y.; Saji, A.; Saka, H. *J. Catal.* **1998**, *178*, 94.
(113) Horikoshi, H.; Kasahara, S.; Fukushima, T.; Itabashi, K.; Okada, T.; Terasaki, O.; Watanabe, D. *J. Chem. Soc. Jpn.* **1989**, 398.
(114) Lohse, U.; Mildebrath, M. *Z. Anorg. Allg. Chem.* **1981**, *476*, 126.
(115) ven Donk, S.; Janssen, A. H.; Bitter, J. H.; de Jong, K. P. *Catal. Rev.* **2003**, *45*, 297.
(116) Janssen, A. H.; Koster, A. J.; de Jong, K. P. *J. Phys. Chem. B* **2002**, *106*, 11905.
(117) Janssen, A. H.; Koster, A. J.; de Jong, K. P. *Angew. Chem., Int. Ed.* **2001**, *40*, 1102.
(118) Dutartre, R.; Menorval, L. C. D.; Di Renzo, F.; McQueen, D.; Fajula, F.; Schulz, P. *Microporous Mater*. **1996**, *6*, 311.
(119) McQueen, D.; Chiche, B. H.; Fajula, F.; Auroux, A.; Guimon, C.; Fitoussi, F.; Schulz, P. *J. Catal.* **1996**, *161*, 587.
(120) Lee, K.-H.; Ha, B.-H. *Microporous Mesoporous Mater*. **1998**, *23*, 211.
(121) Meima, G. R. *CATTECH* **1998**, *2*, 5.
(122) Lago, R. M.; Haag, W. O.; Mikovsky, R. J.; Olson, D. H.; Hellring, S. D.; Schmitt, K. D.; Kerr, G. T. *Stud. Surf. Sci. Catal*. **1986**, *28*, 677.
(123) Rozwadowski, M.; Kornatowski, J.; Włoch, J.; Erdmann, K.; Gołembiewski, R. *Appl. Surf. Sci.* **2002**, *191*, 352.
(124) López-Fonseca, R.; Rivas, B. de.; Gutiérrez-Ortiz, J. I.; González-Velasco, J. R. *Stud. Surf. Sci. Catal*. **2002**, *144*, 717.
(125) Triantafillidis, C. S.; Vlessidis, A. G.; Evmiridis, N. P. *Ind. Eng. Chem. Res.* **2000**, *39*, 307.
(126) Kerr, G. T. *J. Phys. Chem*. **1967**, *71*, 4155.
(127) Katada, N.; Kageyama, Y.; Takahara, K.; Kanai, T.; Begum, H. A.; Niwa, M. *J. Mol. Catal. A* **2004**, *211*, 119.
(128) Beyer, H. K.; Belenyakaja, I. *Stud. Surf. Sci. Catal.* **1980**, *5*, 203.
(129) Scherzer, J. *ACS Symp. Ser*. **1984**, *248*, 157.
(130) Goyvaerts, D.; Martens, J. A.; Grobet, P. J.; Jacobs, P. A. *Stud. Surf. Sci. Catal.* **1991**, *63*, 381.
(131) Corma, A.; Navarro, M. T. *Stud. Surf. Sci. Catal.* **2002**, *142*, 487.
(132) Le Van Mao, R.; Vo, N. T. C.; Sjiariel, B.; Lee, L.; Denes, G. *J. Mater. Chem.* **1992**, *2*, 595.
(133) Kühl, G. H. *J. Phys. Chem. Solids* **1977**, *38*, 1259.
(134) Coster, D.; Blumenfeld, A. L.; Fripiat, J. J. *J. Phys. Chem.* **1994**, *98*, 6201.
(135) Boréave, A.; Auroux, A.; Guimon, C. *Microporous Mater.* **1997**, *11*, 275.
(136) Abbot, J. *Appl. Catal.* **1989**, *47*, 33.
(137) Zholobenko, V. L.; Kustov, L. M.; Kazansky, B. V.; Loeffler. E.; Lohse, U.; Oehman, G. *Zeolites* **1991**, *11*, 132.
(138) Yong, Y.; Gruver. V.; Fripiat, J. J. *J. Catal.* **1994**, *150*, 421.
(139) Schmidt, I.; Madsen, C.; Jacobsen, C. J. H. *Inorg. Chem.* **2000**, *39*, 2279.
(140) Jacobsen, C. J. H.; Houžvicka, J.; Carlsson, A.; Schmidt, I. *Stud. Surf. Sci. Catal.* **2001**, *135*, 167.
(141) Li, Z. J.; Jaroniec, M. *J Am. Chem. Soc*. **2001**, *123*, 9208.
(142) Göltner, C. G. *Angew. Chem., Int. Ed.* **1999**, *38*, 3155.
(143) Sing, K. S. W.; Everett, D. H.; Haul, R. A. W.; Moscou, L.; Pierotti, R. A., Rouquerol, J.; Siemieniewska, T. *Pure Appl. Chem.* **1985**, *57*, 3603.
(144) Schmidt, I.; Krogh, A.; Wienberg, K.; Carlsson, A.; Brorson, M.; Jacobsen C. J. H. *Chem. Commun.* **2000**, 2157.
(145) Janssen, A. H.; Schmidt, I.; Jacobsen, C. J. H.; Koster, A. J.; de Jong, K. P. *Microporous Mesoporous Mater*. **2003**, *65*, 59.
(146) de Jong, K. P.; Geus, J. W. *Catal. Rev. − Sci. Eng*. **2000**, *42*, 481.
(147) Sakthivel, A.; Huang, S.; Chen, W.; Lan, Z.; Chen, K.; Kim, T.; Ryoo, R.; Chiang, A. S. T.; Liu, S. *Chem Mater*. **2004**, *16*, 3168.
(148) Yang, Z.; Xia, Y.; Mokaya, R. *Adv. Mater*. **2004**, *16*, 727.
(149) Tao, Y.; Kanoh, H.; Hanzawa, Y.; Kaneko, K. *Colloids Surf., A* **2004**, *241*, 75.
(150) Carrott, P. J. M.; Sing, K. S. W. *Chem. Ind. (London)* **1986**, *17*, 786.
(151) Bonardet, J.; Fraissard, J.; Unger, K.; Kumar, D.; Ferrero, M.; Ragle, J.; Conner, W. C. *Stud. Surf. Sci. Catal*. **1994**, *87*, 319.
(152) Reichert, H.; Müller, U.; Unger, K. K.; Grillet, Y.; Rouquerol, F.; Rouquerol, J.; Coulomb, J. P. *Stud. Surf. Sci. Catal.* **1991**, *62*, 535.
(153) Llewellyn, P. L.; Coulomb, M. P.; Grillet, Y.; Patarin, J.; Lauter, H.; Reichert, H.; Rouquerol, J. *Langmuir* **1993**, *9*, 1846.
(154) Llewellyn, P. L.; Coulomb, M. P.; Grillet, Y.; Patarin, J.; Lauter, H.; Reichert, H.; Rouquerol, J. *Langmuir* **1993**, *9*, 1852.
(155) Kyriakou, G.; Theocharis, C. R. *Stud. Surf. Sci. Catal.* **2002**, *144*, 709.
(156) Nicholson, D.; Adams, R. W.; Cracknel, R. F.; Papadopoulos, G. K. In *Characterization of Porous Solids IV*; McEnaney, B., Mays, T. J., Rouquerol, J., Rodriguez-Reinoso, F., Sing, K. S. W., Unger, K. K., Eds.; Royal Society of Chemistry: London, 1997; p 57.
(157) Pekala, R. W.; Alviso, C. T.; Kong, F. M.; Hulsey, S. S. *J. Non-Cryst. Solids* **1992**, *145*, 90.
(158) Pekala, R. W.; Alviso, C. T. *Mater. Res. Soc. Symp. Proc.* **1992**, *270*, 3.
(159) Hulsey, S. S.; Alviso, C. T.; Kong, F. M.; Pekala, R. W. *Mater. Res. Soc. Symp. Proc.* **1992**, *270*, 53.
(160) Hanzawa, Y.; Kaneko, K. *Langmuir* **1997**, *13*, 5802.
(161) Bekyarova, E.; Kaneko, K. *Adv. Mater*. **2000**, *12*, 1625.
(162) Hanzawa, Y.; Kaneko, K.; Yoshizawa, N.; Pekala, R. W.; Dresselhaus, M. S. *Adsorption* **1998**, *4*, 187.
(163) Tamon, H.; Ishizaka, H.; Mikami, M.; Okazaki, M. *Carbon* **1997**, *35*, 791.
(164) Hanzawa, Y.; Hatori, H.; Yoshizawa, N.; Yamada, Y. *Carbon* **2002**, *40*, 575.
(165) Tao, Y.; Tanaka, H.; Ohkubo, T.; Kanoh, H.; Kaneko, K. *Adsorpt. Sci. Technol.* **2003**, *21*, 199.
(166) Pekala, R. W.; Coronado, P. R.; Calef, D. F. *Carbon aerogels for hydrogen storage*; US DOE report; U.S. Department of Energy: Washington, DC, 1994; p 227.
(167) Willey, R. J.; Wang, C. T.; Peri, J. B. *J. Non-Cryst. Solids* **1995**, *186*, 408.
(168) Farmer, J. C.; Fix, D. V.; Mack, G. V.; Pekala, R. W.; Poco, J. F. *J. Electrochem. Soc.* **1996**, *143*, 159.
(169) Mayer, S. T.; Pekala, R. W.; Kaschmitter, J. L. *J. Electrochem. Soc*. **1993**, *140*, 446.
(170) Pierre, A. C.; Pajonk, G. M. *Chem. Rev.* **2002**, *102*, 4243.
(171) Al-Muhtaseb, S. A.; Ritter, J. A. *Adv. Mater.* **2003**, *15*, 101.
(172) Tao, Y.; Hattori, Y.; Matsumoto, A.; Kanoh, H.; Kaneko, K. *J. Phys. Chem. B* **2005**, *109*, 194.
(173) Pekala, R. W. *J. Mater. Sci*. **1989**, *24*, 3221.
(174) Qin, G.; Guo, S. *Carbon* **1999**, *37*, 1168.
(175) Yamamoto, Y.; Sugimoto, T.; Suzuki, T.; Mukai, S. R.; Tamon, H. *Carbon* **2002**, *40*, 1345.
(176) Farmer, J. C.; Fix, D. V.; Mack, G. V.; Pekala, R. W.; Poco, J. F. *J. Appl. Electrochem.* **1996**, *26*, 1007.
(177) Ernest, M. V.; Bibler, J. P., Jr.; Whitley, R. D.; Wang, N,-H. L. *Ind. Eng. Chem. Res.* **1997**, *36*, 2775.
(178) Glora, M.; Wiener, M.; Petricevic, R.; Probstle, H.; Fricke, J. *J. Non-Cryst. Solid* **2001**, *285*, 283.
(179) Petricevic, R.; Glora, M.; Fricke, J. *Carbon* **2001**, *39*, 857.
(180) Frackowiak, E.; Beguin, F. *Carbon* **2001**, *39*, 937.
(181) Huang, B.; Huang, Y.; Wang, Z.; Chen, L.; Xue, R.; Wang, F. *J. Power Sources* **1996** *58*, 231.
(182) Tao, Y.; Kanoh, H.; Kaneko, K. *Langmuir* **2005**, *21*, 504.
(183) Weisz, P. B. *Chemtech* **1973**, 498.
(184) Corma, A. *Stud. Surf. Sci. Catal*. **1989**, *49*, 49.
(185) Corma, A.; Fornes, V.; Pergher, S. B.; Maesen, Th. L. M.; Buglass, J. G. *Nature* **1998**, *396*, 353.
(186) van Donk, S.; Bitter, J. H.; Verberckmoes, A.; Versluijs-Helder, M.; Broersma, A.; de Jong, K. P. *Angew. Chem., Int. Ed.* **2005**, *44*, 1360.
(187) Hartmann, M. *Angew. Chem., Int. Ed.* **2004**, *43*, 5880.

(188) Christensen, C. H.; Johannsen, K.; Schmidt, I.; Christensen, C. H. *J. Am. Chem. Soc.* **2003**, *125*, 13370.
(189) Christensen, C. H.; Schmidt, I.; Christensen, C. H. *Catal. Commun.* **2004**, *5*, 543.
(190) Tromp, M.; van Bokhoven, J. A.; Garriga Oostenbrink, M. T.; Bitter, J. H.; de Jong, K. P.; Koningsberger, D. C. *J. Catal.* **2000**, *190*, 209.
(191) Meima, G. R. *CATTECH* **1998**, *2*, 5.
(192) Corma, A.; Martínez, A.; Arroyo, P. A.; Monteiro, J. L. F.; Sousa-Aguiar, E. F. *Appl. Catal. A* **1996**, *142*, 139.
(193) Gheorghiu, S.; Coppens, M.-O. *AIChE J.* **2004**, 50812.
(194) Venuto, P. B. *Stud. Surf. Sci. Catal.* **1996**, *105*, 811.
(195) Chiche, B.; Sauvage, E.; Direnzo, F.; Ivanova, I. I.; Fajula, F. *J. Mol. Catal. A: Chem.* **1998**, *134*, 145.
(196) Corma, A. *J. Catal*. **2003**, *216*, 298.
(197) Tabata, T.; Ohtsuka, H. *Catal. Lett*. **1997**, *48*, 203.
(198) Christensen, C. H.; Schmidt, I.; Carlsson, A.; Johannsen, K.; Herbst, K. *J. Am. Chem. Soc.* **2005**, *127*, 8098.
(199) Olivas, A.; Jerdev, D. I.; Koel, B. E. *J. Catal*. **2004**, *222*, 285.
(200) Besenbacher, F.; Chorkendorff, I.; Clausen, B. S.; Hammer, B.; Molenbroek, A. M.; Nørskov, J. K.; Stensgaard, I. *Science* **1998**, *279*, 1913.
(201) Pekala, R. W.; Alviso, C. T. *Mater. Res. Soc. Symp. Proc.* **1990**, *180*, 791.
(202) Raman, V. I.; Palmese, G. R. *Colloids Surf., A* **2004**, *241*, 119.
(203) Davis, M. E. *Stud. Sci. Catal.* **1995**, *97*, 35.
(204) Helmkamp, M. M.; Davis, M. E. *Annu. Rev. Mater. Sci.* **1995**, *25*, 162.
(205) Tao, Y.; Kanoh, H.; Kaneko, K. *Adv. Mater*. **2005**, *17*, 2789.

CR040204O